FE nonlinear analysis of lateral-torsional buckling resistance

J. Valeš, Z. Kala, J. Martinásek and A. Omishore

***Abstract*—** The article focuses on the analysis of the effects of stability phenomena on the ultimate limit state of a steel beam subjected to uniform bending moment along its length. The key parameters that influence the load carrying capacity include imperfections and slenderness. The elastic and inelastic resistance obtained using the nonlinear finite element method were compared with analytical and standardised approaches in the article. The effects of warping of the end sections on the resistance and reliability of steel beams is studied. For this purpose, bending of the beam was introduced, firstly with forces on the end sections, and secondly by rotating the end sections.

***Keywords*—** Static, resistance, steel, beam, lateral torsional buckling, stability, imperfections, sensitivity, reliability.

I. Introduction

Thin-walled slender members constitute an important part of load bearing steel structures, which are effective in terms of both weight and optimal load transfer [1]. Engineers can choose from a wide range of thin walled steel members, the profiles of which are optimized with regard to the required load bearing characteristic.

A leading example for this specific load bearing characteristic of thin-walled members is the classical I-beam. An I-beam is a beam with an I or H-shaped cross-section. I-beams made from structural steel are, due to their load bearing properties, widely used in construction and civil engineering. The cross-section comprises of the flanges and the web. If the beam is subjected to transverse loads in the plane of the web, the flanges have a dominant share in resisting bending and the web ensures the distribution of the shear forces. Stiffness of the steel I-beam is maximum if the beam is subjected to bending about the major axis, see Fig. 1. This high bending stiffness is determined by the location of most of the material in the flanges far from its neutral axis, resulting in high compression in one of the flanges and high tension in the other flange. The compressed flange has a tendency to buckle, while the tensed flange partially stabilizes this process. The process of buckling leads to secondary bending around the minor axis accompanied by rotation around the beam axis. This is collectively known as lateral-torsional buckling. The further the flanges are from each other, the greater the contribution of lateral-torsional buckling to the reduction of the resistance of the I-beam [2].

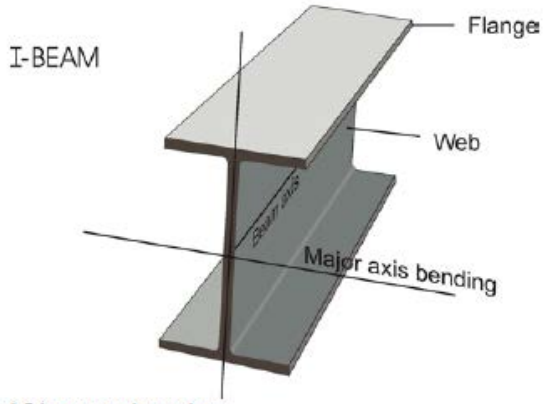

Fig. 1 I-beam steel member

If the I-beam is high, its resistance is also reduced by buckling of the thin walls and flanges. Typical examples are beams welded from thin walls [3, 4]. If the slender compressed walls get to an unstable equilibrium position from a stable equilibrium position due to the action of very small forces, the cross-section becomes unstable and is not very effective in the transfer of internal forces. Loss of stability is accompanied by increased sensitivity of the stress state of the beam to initial imperfections, which has an adverse effect on the resistance of the beam [5]. For these reasons, increasing the bending stiffness by relocating material farther from the neutral axis is only effective to a certain extent. Thus, great caution is recommended whilst designing high welded I-beams.

The geometry of mass produced European steel hot rolled I-sections are designed so that the beam transfers bending optimally and local loss of stability of slender walls or flanges of the section occur minimally. EUROCODE 3 [6] classifies European hot rolled I-beams as first class beams, for which the probability of failure due to buckling of the web or flange is very small in comparison with other sources of failure.

This result was achieved with the financial support of the projects GA ČR 14–17997S.

Jan Valeš is with the Brno University of Technology, Faculty of Civil Engineering, Brno, 602 00 CZ (phone: +420-541147116; fax: +420-541147392; e-mail: vales.j@fce.vutbr.cz).

Zdeněk Kala is with the Brno University of Technology, Faculty of Civil Engineering, Brno, 602 00 CZ (phone: +420-541147382; fax: +420-541147392; e-mail: kala.z@fce.vutbr.cz).

Josef Martinásek is with the Brno University of Technology, Faculty of Civil Engineering, Brno, 602 00 CZ (phone: +420-541147378; fax: +420-541147392; e-mail: martinasek.j@fce.vutbr.cz).

Abayomi Omishore is with the Brno University of Technology, Faculty of Civil Engineering, Brno, 602 00 CZ (phone: +420-541147131; fax: +420-541147392; e-mail: omishore.a@fce.vutbr.cz).

Initial geometric imperfections of mass produced European hot rolled I-beams are usually modelled acc. to the first eigenmode of buckling [7]. This form, however, may not be in full compliance with results of experimental research and the probabilistic approach [8]. Initial imperfections of hot rolled steel I-beams arise mainly during production [9]. Hot rolled steel I-beams are biaxially symmetrical and cooling also takes place symmetrically, however, unevenly across the cross-section. The slight asymmetry of the I-beam due to imperfections of the cross-section is of little significance and can be neglected in static tasks [9]. Hot rolling and cooling of hot rolled steel I-beams generally does not yield initial geometric imperfections associated with buckling or lateral buckling. The eigenmodes are related to loss of stability due to loading of the beam and is not related to the process of rolling and cooling.

Research of the limit states of slender steel beams has developed from Vlasov's theory of thin-walled beams [10-12] to modern nonlinear finite element models (FEM) [13-15]. Modern numerical simulations based on nonlinear FEM allow the consideration of a number of material models [16] and geometric initial imperfections [17, 18].

Analysis of safety and reliability of building structures has an important role in multiple-criteria decision analysis [19-22]. The introduction of initial imperfections acc. to the first eigenmodes by designers has its justification in reliability analysis, which is a common part of verification procedures of standards for design [23, 24].

Analysis of the limit states of steel I-beams based on the non-linear FEM is a very complex problem, the solution of which requires processing of a lot of information. Stability problems of beams with imperfections, such as geometrical and material imperfections, should be investigated with both geometrical and material nonlinear solution. The more advanced the FEM, the more numerical data must be entered as software inputs. The objective of this article is to study the ultimate limit state due to inelastic lateral–torsional buckling.

II. Computational Model

Profile I200 is depicted in Fig. 2a. The computational model was created using an idealized geometry, see Fig. 2b. Geometric characteristics of the profile include the cross-section height h, width b, web thickness t_1, flange thickness t_2.

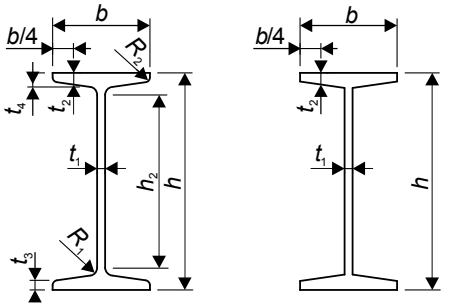

Fig. 2 profile I200: (a) real, (b) idealized

A. The Beam Theory

The curvature of the beam axis was introduced in the shape of a half sine wave (1), which corresponds to the first eigenmode of lateral beam buckling.

$$v_0 = a_{v_0} \sin\left(\frac{\pi\ x}{L}\right), \quad \varphi_0 = a_{\varphi_0} \sin\left(\frac{\pi\ x}{L}\right) \tag{1}$$

Initial curvature of the axis of amplitude v_0 is accompanied by initial rotation φ_0 of the cross-section around the x-axis. Both amplitudes v_0 and φ_0 are defined using sine functions, see Fig. 3.

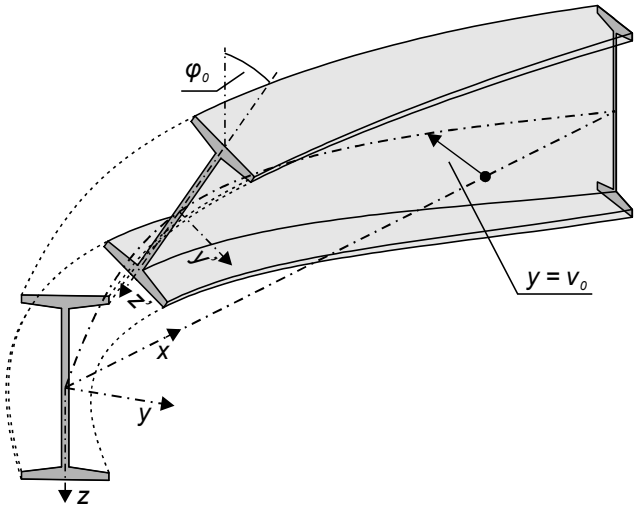

Fig. 3 initial axis imperfection

If the beam is curved according to the first eigenmode, it holds for amplitudes a_{v0} and $a_{\varphi 0}$ that

$$a_{v0} = a_{\varphi 0} \frac{M_{cr} L^2}{\pi^2 E I_z}, \quad a_{\varphi 0} = e_0 \frac{2\pi^2 E I_z}{2 M_{cr} L^2 + \pi^2 h E I_z} \tag{2}$$

where e_0=L/1000 is the imperfection related to the upper edge of the cross-section, h is the cross-section height, I_z is the second moment of area around axis z, L is the beam length, E is the Young's modulus of elasticity and M_{cr} is the elastic critical moment at lateral beam buckling. The elastic behaviour of beams can be analyzed using two differential equations [25]:

$$E I_z \frac{\partial^2 v}{\partial x^2} + M\left(\varphi + \varphi_0\right) = 0 \tag{3}$$

$$E I_\omega \frac{\partial^3 \varphi}{\partial x^3} - G I_t \frac{\partial \varphi}{\partial x} + M\left(\frac{\partial v}{\partial x} + \frac{\partial v_0}{\partial x}\right) = 0 \tag{4}$$

where I_t is the torsion constant, I_ω is the warping constant and G is the shear modulus. The beam is considered as simply supported and loaded at both ends by equal bending moment of opposite sense. For such a loading case, the relation for M_{cr}

can be derived acc. to [1, 7, 25], in the form

$$M_{cr} = \frac{\pi}{L}\sqrt{EI_z\, GI_t}\,\sqrt{1+V^2} \tag{5}$$

with

$$V = \frac{\pi}{L}\sqrt{\frac{EI_\omega}{GI_t}} \tag{6}$$

B. Finite Element Model

Computational models were created with the Ansys software, using the 3D element SOLID185 [26]. The loading on the edge cross-section of the 3D model was created in two ways: firstly, as pairs of forces in the cross-section nodes. The forces act perpendicularly to the end cross-section, and so, their arms remain constant, see Fig. 4 (a). Secondly, the loading was created as rotations about *y*-axis in the cross-section nodes, see Fig. 4 (b). The corresponding value of bending moment was taken as the sum of node reactions.

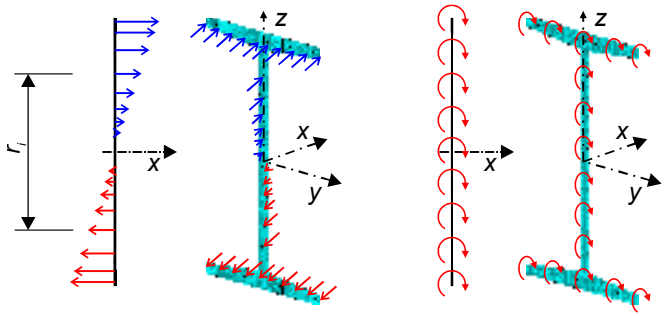

Fig. 4 loading: (a) as pairs of forces, (b) as rotations about axis *y*

I-beams are usually modelled using beam or shell elements. Modern beam elements tak into account St. Venant torsion as well as warping torsion and bimoment [27]. Beam elements are primarily adapted for elastic analysis; inelastic analysis requires advanced FE modelling elements Shell or Solid.

Shell elements are often used to model prismatic IPE sections. Shell elements allow the study of elastic and inelastic resistance of beams with consideration to a large number of imperfections.

In the presented study the beam I200 was meshed using spatial elements defined in the Ansys software [26] as SOLID185. Element SOLID185 allows detailed analysis of all forementioned phenomena. SOLID185 is an element with eight nodes that can be used for 3D modelling of solid structures with plasticity, hyperelasticity, stress stiffening, creep, large deflection, and large strain capabilities. Each node has three degrees of freedom, i.e. translations in the nodal *x*, *y*, and *z* directions. The element was set as a homogeneous structural solid element. The enhanced strain formulation, which prevents shear locking in bending-dominated problems and volumetric locking in most incompressible cases, was considered. The formulation introduces a certain number of internal and inaccessible degrees of freedom to overcome shear locking, and an additional internal degree of freedom for volumetric locking (apart from the case of plane stress in 2-D elements). All internal degrees of freedom are introduced automatically at the element level and condensed out during the solution phase of the analysis [26].

The computational model is illustrated in Fig. 5 and Fig. 6 with the initial imperfections shown in a magnified scale.

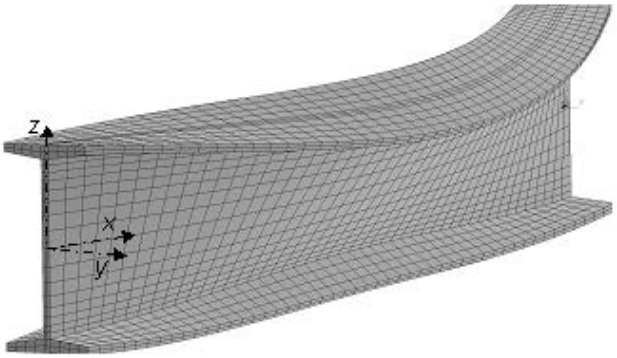

Fig. 5 computational model in Ansys – axonometry

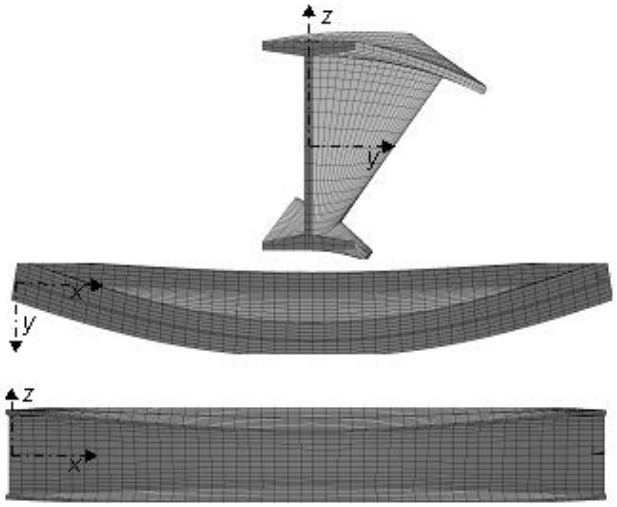

Fig. 6 computational model in Ansys – views

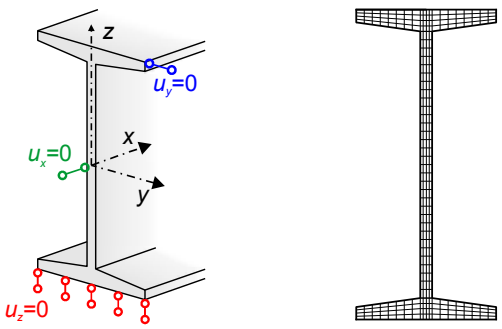

Fig. 7 (a) boundary conditions, (b) cross-section mesh

Boundary conditions are set so that the edge cross-sections can warp, see Fig. 7 (a). The support in the direction of x-axis $u_x = 0$ is introduced at one end only. The meshed cross-section is shown in Fig. 7 (b).

Evaluation was performed using an elastic-plastic stress-strain diagram without hardening acc. to the standard [6], see Fig. 8. The value of yield strength f_y was considered by its nominal value 235 MPa.

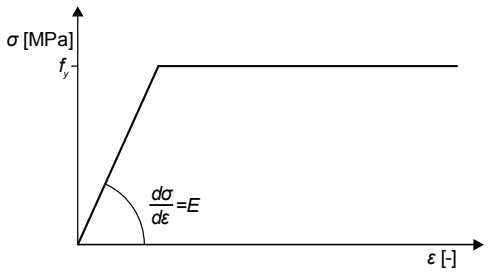

Fig. 8 bilinear stress-strain diagram

C. Analytical Solution of Elastic Resistance

The elastic resistance M_R of the beam can be derived from equations (3) and (4). M_R represents the bending moment at which the maximum value of the von Mises stress corresponds to yield strength f_y of the steel [6], and is given by the relation (7):

$$M_R = -\frac{\sqrt{4Q_1(Q_4 - 2M_{cr}Q_3 + Q_1) + (Q_4 + Q_5)^2}}{4M_{cr}W_z} + \frac{2Q_1 + Q_4 + Q_5}{4M_{cr}W_z} \tag{7}$$

where

$$\begin{aligned} Q_1 &= M_{cr}W_yW_zf_y \\ Q_2 &= M_{cr}W_z + P_zW_y|a_{v0}| \\ Q_3 &= M_{cr}W_z - P_zW_y|a_{v0}| \\ Q_4 &= 2P_z^2I_y|a_{v0}| \\ Q_5 &= 2M_{cr}Q_2 \\ P_z &= \pi^2\frac{EI_z}{L^2} \end{aligned} \tag{7a}$$

W_y is the cross-section module to y-axis, and W_z is the cross-section module to z-axis.

For the calculation of the plastic resistance $M_{pl,R}$, it is possible to apply, by means of (7), the empirical relation according to [28]

$$M_P = M_R\frac{W_{pl,y}}{W_y}\alpha + M_R(1-\alpha) \tag{8}$$

where

$$\alpha = \left(\frac{1}{1+\bar{\lambda}_{LT}^4}\right)^4 \tag{9}$$

is the non-dimensional slenderness (10) at lateral beam buckling according to [6]

$$\bar{\lambda}_{LT} = \sqrt{\frac{W_{pl,y}f_y}{M_{cr}}} \tag{10}$$

where $W_{pl,y}$ is the plastic cross-section module to y-axis. Cross-section characteristics of the idealized profile I200 according to Fig. 2 (b) are given in Table I.

TABLE I
CROSS-SECTION CHARACTERISTICS

Characteristic	Symbol	Value
Cross-section height	h	0.200 m
Cross-section width	b	0.090 m
Web thickness	t_1	0.0075 m
Flange thickness	t_2	0.0113 m
Second moment of area about y	I_y	21.235E-6 m^4
Second moment of area about z	I_z	1.188E-6 m^4
Torsion constant	I_t	1.187E-7 m^4
Warping constant	I_ω	1.017E-8 m^6
Section modulus about axis y	W_y	21.235E-5 m^3
Section modulus about axis z	W_z	2.639E-5 m^3
Plastic section modulus about y	$W_{pl,y}$	24.684E-5 m^3

D. Resistance According to Eurocode 3

The design resistance moment of a horizontally unsupported beam at lateral beam buckling $M_{b,Rd}$ is determined from the relation

$$M_{b,Rd} = \chi_{LT}\frac{W_yf_y}{\gamma_{M1}} \tag{11}$$

The cross-section I200 is a cross-section of Class 1, and therefore, the cross-section module W_y can be determined as $W_y = W_{pl,y}$, see Table I. The partial resistance factor of cross-section when evaluating the stability $\gamma_{M1} = 1.0$. Reduction factor for lateral-torsional buckling χ_{LT} for the appropriate slenderness may be determined from

$$\chi_{LT} = \frac{1}{\Phi_{LT} + \sqrt{\Phi_{LT}^2 - \bar{\lambda}_{LT}^2}} \tag{12}$$

in which

$$\Phi_{LT} = 0.5\left[1 + \alpha_{LT}(\bar{\lambda}_{LT} - 0.2) + \bar{\lambda}_{LT}^2\right] \tag{13}$$

The curve of lateral beam buckling b can be used for the cross-section I200. The value of imperfection factor for lateral-torsional buckling is $\alpha_{LT} = 0.34$ [6].

E. Resistance of Finite Element Model

Geometric and material nonlinear solution available in the Ansys software was used to calculate the inelastic resistance. The inelastic resistance was determined as the maximum loading moment of the beam, during which the determinant of the stiffness matrix is close to zero and the calculation is a step from the diverging solution.

Inelastic resistance $M_{pl,ANSYS,B}$ is defined as the peak of the curve, see Fig. 9. The loading moment was created by rotating the end sections. Rotation was perfomed incrementally, step by step. The points on the curves corresponding to the inelastic resistance are depicted in Fig. 9.

Inelastic resistance $M_{pl,ANSYS,A}$ is defined similarly, with the difference that the ends of the beam are loaded by moment, see Fig. 4a.

The elastic resistance $M_{R,Ansys}$ is obtained upon reaching the prescribed stress (of yield strength f_y) in any point of the beam.

With regard to the plane symmetry of the beam along the plane passing through its centre and parallel with *yz* the yield strength is reached in one of the cross-section tops mid-span of the beam. Linear regression was performed using a small data set including the value of the moment loading to accurately quantify the elastic resistance, and the corresponding value of the von Mises stress near the yield strength. A seventh degree polynomial was applied as the basic linear regression model with negligible absolute error.

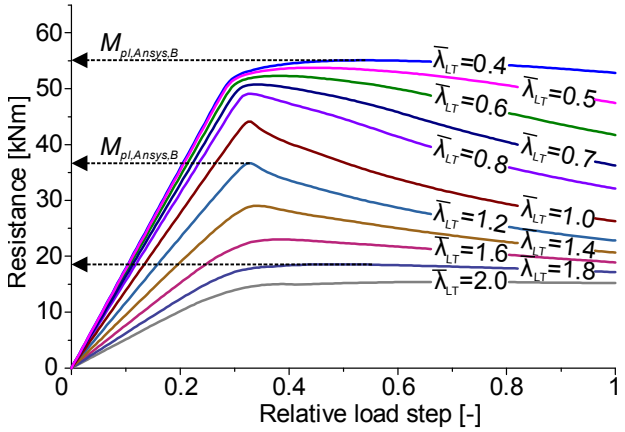

Fig. 9 graph of corresponding plastic resistance $M_{pl,Ansys,B}$ for a set of non-dimensional slendernesses

III. Comparison of Resistances

The values of analytically computed resistances according to (7), (8) and (11) are depicted by the curves in Fig. 10. The diagram is completed by the Euler hyperbola (5), and the values of resistance M_d given by the relation

$$M_d = f_y W_{pl,y} \tag{14}$$

The range of non-dimensional slenderness $\bar{\lambda}_{LT}$ is from 0 to 2.1. Taking into account (10) and (5) the non-dimensional slenderness can be calculated from the function in dependence on the beam length L. The maximum length of the beam was considered as 12 meters. Thus, the relation for the dependence of length on non-dimensional slenderness can be derived in the form

$$L = \pi \sqrt{\frac{\bar{\lambda}_{LT}^2 I_z^{0.5} 2EI_\omega}{D^{0.5} - \bar{\lambda}_{LT}^2 I_z^{0.5} GI_t}} \tag{15}$$

in which

$$D = \bar{\lambda}_{LT}^4 G^2 I_t^2 I_z + 4 f_{y,n}^2 W_{pl,y}^2 I_\omega \tag{16}$$

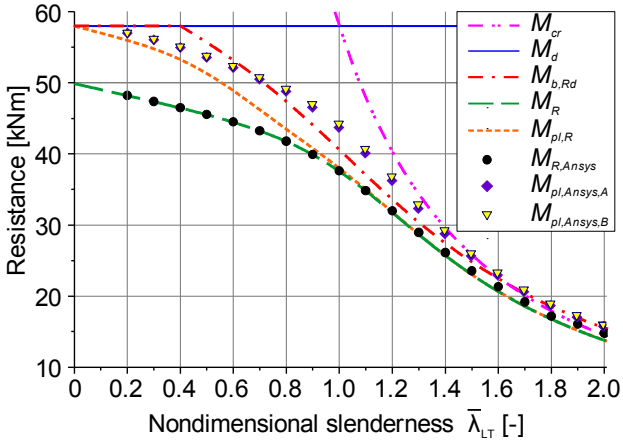

Fig. 10 graph of corresponding plastic resistance *Mpl,Ansys,B* for a set of non-dimensional slendernesses

Due to the non-linear relation between $\bar{\lambda}_{LT}$ and L, the resistance is also laid out to the beam length, see. Fig. 11.

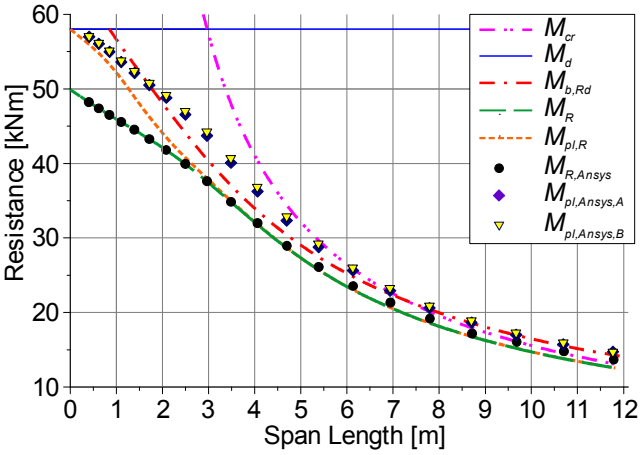

Fig. 11 Diagram of resistance vs. span length

Obtained resistance values $M_{pl,Ansys,A}$ and $M_{pl,Ansys,B}$ are practically the same, although $M_{pl,Ansys,B}$ gives less than 2 % higher values.

IV. Stress of the Beam under Ultimate Limit State

The nonlinear FEM model allows a very detailed study of the stress of beams under limit states. Fig. 12 a) shows the longitudinal stress midspan of the beam from $M_{R,Ansys}$. The stress has a linear course and reaches the value of 235 MPa at the endpoints of the section. The beam can be loaded from $M_{R,Ansys}$ to $M_{pl,Ansys,A}$ (or $M_{pl,Ansys,B}$), where stress state acc. to Fig. 2b. is reached. It is apparent from Fig. 10 that the absolute difference between resistance $M_{pl,Ansys}$ and the resistance $M_{R,Ansys}$ increases with decreasing slenderness values. On the contrary, the higher the slenderness the more negligible the difference.

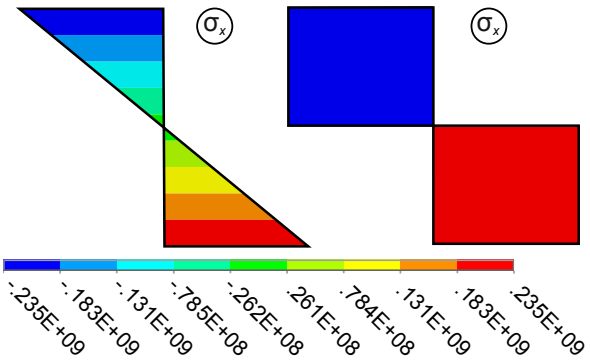

Fig. 12 stress course in web σ_x at reaching (a) elastic resistance, (b) plastic resistance

The cross-section can theoretically plasticize according to Fig. 12 (b). This approach leads to the formation of a plasic hinge and is an important part of numerous optimization analyses [29, 30]. However, the reality is such that even for the lowest considered values of slenderness, the cross-section of the beam need not plasticize fully upon reaching the total resistance. Such a case of stress distribution σ_x is observed, for e.g., for the slenderness $\overline{\lambda}_{LT}$ =0.6, illustrated in Fig.13.

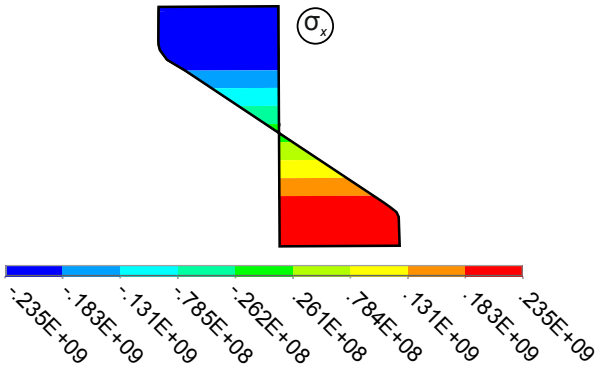

Fig. 13 stress course in web σx for slenderness 0.6 at reaching the total resistance

Fig. 14 and Fig. 15 can be used to compare von Mises stress distributions for both cases of beam loading with end moments acc. to Fig. 4. The limit state of beams loaded by moments $M_{pl,Ansys,A}$ (loading acc. to Fig. 4a) and $M_{pl,Ansys,B}$ (loading acc. to Fig. 4b) was studied. There is no significant difference in the stress distributions arising from both types of loading.

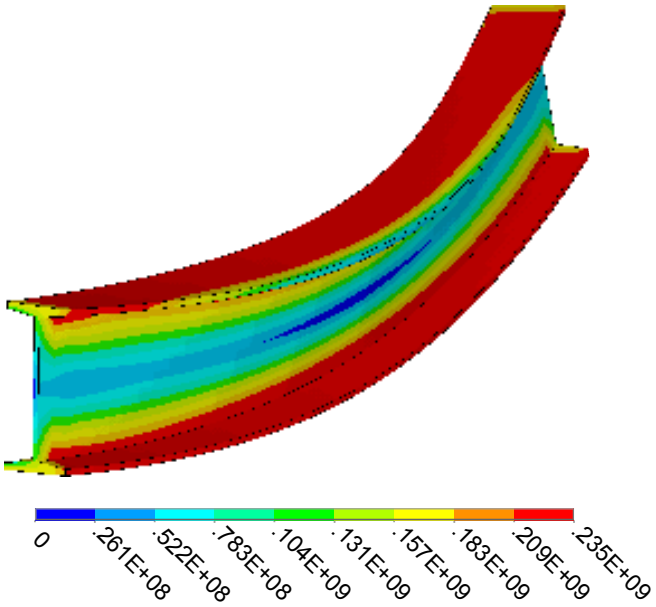

Fig. 14 von Mises stress σ_{vM} in the beam for slendernes 0.6 at reaching the total resistance – loading by pairs of forces

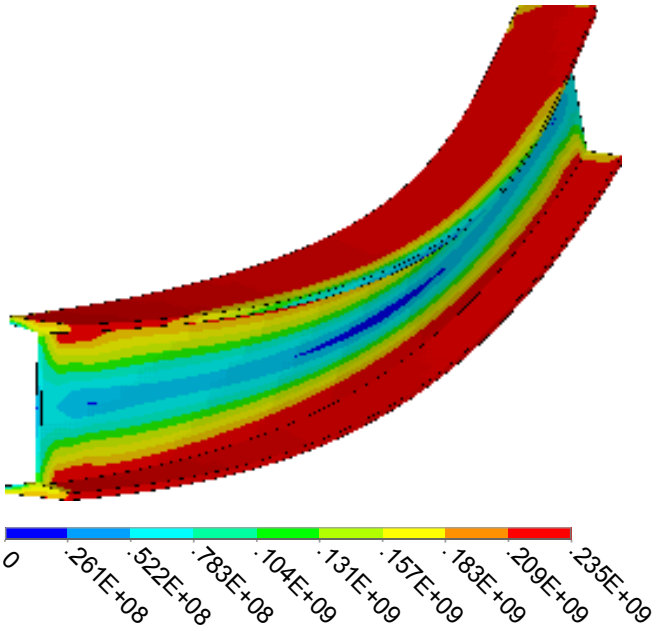

Fig. 15 von Mises stress σ_{vM} in the beam slenderness 0.6 at reaching the total resistance – loading by rotations

V. Conclusion

Several approaches for the calculation of the elastic and inelastic resistance were compared in the article. The elastic resistance $M_{R,Ansys}$ calculated using FEM and the Ansys program completely agrees with the resistance $M_{R,Ansys}$ calculated analytically in the closed form, which was derived in [7, 31]. It is evident from Fig. 10 that with increasing

slenderness the elastic and inelastic resistance obtained both analytically and using the FEM approach Euler's hyperbola and the task becomes a stability problem.

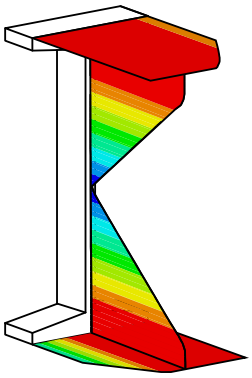

Fig. 16 von Mises stress σ_{vM} cross-section in the span middle for slenderness 0.6 at reaching the total resistance

A good agreement is apparent from the comparison of the standard resistance $M_{b,Rd}$ and resistance $M_{pl,Ansys}$ calculated using the FEM approximately for slenderness $\overline{\lambda}_{LT} \geq 0.7$. For $\overline{\lambda}_{LT} < 0.7$, the standard resistance is by 2 – 6 % higher. The resistance $M_{pl,R}$ evaluated acc. to the empirical formula (8) is less than $M_{b,Rd}$ and $M_{pl,Ansys}$ and provides a safe estimate based on the elastic resistance M_R. The analysis of the influence of residual stress on the ultimate limit state will be the subject of further research. Nonlinear FEM is a very powerful tool, which can be used to study safety and reliability of load bearing steel structures.

ACKNOWLEDGMENT

The article was elaborated within the framework of project GAČR 14-17997S.

REFERENCES

[1] T. V. Galambos, *Stability Design Criteria for Metal Structures*. John Wiley and Sons, Ltd., 1998, p. 911.

[2] D. Schillinger, "Stochastic FEM based stability analysis of I-sections with random imperfections," M.S. thesis, Stuttgart University, 2008, p.93,

[3] Z. Kala, J. Kala, M. Škaloud, and B. Teplý, "Sensitivity analysis of the effect of initial imperfections on the (i) ultimate load and (ii) fatigue behaviour of steel plate girders," *Journal of Civil Engineering and Management*, vol. 11, no. 2, pp. 99–107, 2005.

[4] Z. Kala, J. Kala, "Resistance of thin-walled plate girders under combined bending and shear," *WSEAS Transactions on Applied and Theoretical Mechanics*, vol. 4, no. 5, pp. 242–251, 2010.

[5] J. Zahn, "Lateral stability of beams with initial imperfections," *Journal of Engineering Mechanics*, vol. 109, no. 3, pp. 821–835, 1983.

[6] EN 1993-1-1 Design of Steel Structures - Part 1-1: General rules and rules for buildings, CEN Brussels, 2006.

[7] Z. Kala, "Elastic lateral-torsional buckling of simply supported hot-rolled steel I-beams with random imperfections," *Procedia Engineering*, vol. 57, pp. 504–514, 2013.

[8] J. Szalai, F. Papp, "On the probabilistic evaluation of the stability resistance of steel columns and beams," *Journal of Constructional Steel Research*, vol. 65, no. 3, pp. 569–577, 2009.

[9] Z. Kala, J. Melcher, L. Puklický "Material and geometrical characteristics of structural steels based on statistical analysis of metallurgical products," *Journal of Civil Engineering and Management*, vol. 15, no. 3, pp. 299–307, 2009.

[10] V.Z. Vlasov, *Thin-walled elastic beams*. 2nd ed. Israel Program for Scientific Translations, Jerusalem, 1961.

[11] J. Jönsson, "Distortional warping functions and shear distributions in thin-walled beams," *Thin-Walled Structures*, vol. 33, no. 3, pp. 245–268, 1999.

[12] J. Jönsson, "Distortional theory of thin-walled beams," *Thin-Walled Structures*, vol. 33, no. 4, pp. 269–303, 1999.

[13] Z. Kala, J. Kala, "Sensitivity analysis of stability problems of steel structures using shell finite elements and nonlinear computation methods," *WSEAS Transactions on Applied and Theoretical Mechanics*, vol. 4, no. 3, pp. 105–114, 2009.

[14] Z. Kala, J. Kala, and A. Omishore, "Probabilistic Buckling Analysis of Thin-Walled Steel Columns Using Shell Finite Elements," *International Journal of Mechanics*, vol. 10, pp. 213–218, 2016.

[15] O. Sucharda, J. Vasek, and J. Kubosek, "Elastic-plastic calculation of a steel beam by the finite element method," *International Journal of Mechanics*, vol. 9, pp. 228–235, 2015.

[16] F. Hokes, J. Kala, and O. Krnavek, "Nonlinear Numerical Simulation of a Fracture Test with Use of Optimization for Identification of Material Parameters," *International Journal of Mechanics*, vol. 10, pp. 159–166, 2016.

[17] P. Panedpojaman, W. Sae-Long, T. Chub-uppakarn, "Cellular beam design for resistance to inelastic lateral–torsional buckling," *Thin-Walled Structures*, vol. 99, pp. 182–194, 2016.

[18] J. Valeš, Z. Kala, J. Martinásek, "Solving lateral beam buckling problems by means of solid finite elements and nonlinear computational methods," *International Journal of Mathematical and Computational Methods*, vol. 1, pp. 103–108, 2016.

[19] J. Xu, Q. Liu, X. Lei, "A fuzzy multi-objective model and application for the discrete dynamic temporary facilities location planning problem," *Journal of Civil Engineering and Management*, vol. 22, no. 3, pp. 357–372, 2016.

[20] J. Antucheviciene, Z. Kala, M. Marzouk, E.R. Vaidogas, "Solving civil engineering problems by means of fuzzy and stochastic MCDM methods: Current state and future research," *Mathematical Problems in Engineering*, vol. 2015, Article ID 362579, p. 16, 2015.

[21] J. Antucheviciene, Z. Kala, M. Marzouk, E.R. Vaidogas, "Decision making methods and applications in civil engineering," *Mathematical Problems in Engineering*, vol. 2015, Article ID 160569, p. 3, 2015.

[22] E.K. Zavadskas, D. Kalibatas, D. Kalibatiene, "A multi-attribute assessment using WASPAS for choosing an optimal indoor environment," *Archives of Civil and Mechanical Engineering*, vol. 16, no. 1, pp. 76–85, 2016.

[23] M. Kala, "Global sensitivity analysis in stability problems of steel frame structures," *Journal of Civil Engineering and Management*, vol. 22, no. 3, pp. 417–424, 2016.

[24] A. Omishore, "Verification of design procedures of structural stability using probabilistic methods of reliability analysis," *AIP Conference Proceedings*, vol. 1479, pp. 2082–2085, 2012.

[25] N.S. Trahair, The Behaviour and Design of Steel Structures. John Wiley and Sons, Ltd., 1977, p. 320.

[26] ANSYS Theory Release 15.1, ANSYS Inc., 2014.

[27] J. Valeš, "Effect of random axial curvature on the performance of open and closed section steel columns," *AIP Conference Proceedings*, vol. 1558, pp. 2512–2515, 2013.

[28] Z. Kala, "Reliability analysis of the lateral torsional buckling resistance and the ultimate limit state of steel beams with random imperfections," *Journal of Civil Engineering and Management*, vol. 21, no. 7, pp. 902–911, 2015.

[29] J. Atkočiūnas, T. Ulitinas, S. Kalanta, G. Blaževičius, "An extended shakedown theory on an elastic–plastic spherical shell," *Engineering Structures*, vol. 101, pp. 352–363, 2015.

[30] V. Jankovski, J. Atkočiūnas, "Biparametric shakedown design of steel frame structures," *Mechanika*, vol. 17, No. 1, pp. 5–12, 2011.

[31] Z. Kala, "Sensitivity and reliability analyses of lateral-torsional buckling resistance of steel beams," *Archives of Civil and Mechanical Engineering*, vol. 15, no. 4, pp. 1098–1107, 2015.